Improved impedance conditions for a thin layer problem in a non smooth domain*

Alexis Auvray and Grégory Vial†

April 13, 2018

Abstract

In this article, we consider the model problem of the Laplace equation in a domain with a thin layer on a part of its boundary. The singularities appearing where boundary conditions change deteriorates the efficiency of the classical impedance condition used to replace the layer. Modified impedance conditions are proposed, which lead to some improvements in the error estimates.

1 Introduction

Problems involving materials with thin structures arise in various application fields. This is the case for the analysis of mechanical properties of thin rods, beams, plates, or shells for which reduced models are derived, allowing to deal with lower dimensional geometries without thickness. We will focus in this paper on problems where the thin structure lies *around* another material, or *inside* materials, and has significantly different properties. We have in mind a large variety of applications. In mechanical engineering, the study of the properties of composite materials is a critical issue, see [29, 30], with the reinforcement by thin fibers or layers. Situations where two materials are glued together enter this scope as well, see e.g. [31]. For electromagnetism, thin dielectric layers appear in many situations, see for example [34] for the eddy current problem in the context of copper deposites on tubes, or [55] for the skin effect problem, which has strong connections with thin layers. Biological tissues often involve thin parts, see [42] for a mathematical and numerical study of the electromagnetic field around and inside a biological cell, or [20] for the description of the diffusion Magnetic Resonance Imaging signal in biological tissues. Thin films are good examples as well, and various models have to be considered depending on their nature and size, see [47] and the references therein for falling films, or [50] for an electrochemical situation. We can mention large scale applications in geophysics, where the earth crust may be considered as a thin layer, see [15, 45]. This list is not exhaustive and many other applications could be cited.

The common issue raised by such problems is the following. If we completely omit the thin layer in the (analytical or numerical) study, the obtained solution may significantly differ from the expected one. On the other hand, incorporating directly the thin layer generally prevents from analytical results, and leads to serious difficulties in the numerical simulations. Indeed, the discretization of the domain needs a local refinement at the scale of the layer, and due to the number of degrees of freedom, the computation can become cumbersome, especially for three-dimensional

*This article has been partially supported by the Projects ARAMIS (ANR-12-BS01-0021) and OPTIFORM (ANR-12-BS01-0007).

†Univ Lyon, École centrale de Lyon, CNRS UMR 5208, Institut Camille Jordan, F-69134 Écully, France.

problems. An alternative solution consists in replacing the initial transmission problem with an approximate model, where the thin layer no longer appears, but is replaced with a suitable *approximate boundary condition* – or *approximate interface condition*, depending whether the layer lies inside or around the medium – also referred as to *effective boundary condition* (or *impedance condition* in electromagnetics).

This strategy has generated a large amount of mathematical studies for both the derivation, the justification, and the analysis of such approximate boundary conditions. During the nineties, many geometrical situations have been investigated, from the simplest problem of a layer with uniform thickness around a material [28, 11], or non-uniform thickness layers [5], to the more general case of periodically oscillating layers [3, 38] (wall laws for flows over rough surfaces) or [6] (scattering by thin periodic coatings). Likewise, different models have been considered: stationary Laplace-Dirichlet and Helmholtz problems in [28, 11], harmonic Maxwell equations in [28, 5], time dependent Maxwell problem in[35], Stokes system in [3, 38]. Let us finally mention some works which directly consider the thin layer problem, and develop adapted numerical strategies [32, 19], and a nice paper on the problem of optimizing the thickness function [2].

The subject still generates active research activities. Let us mention [1, 10, 14] for mechanical applications, [12, 48, 42] for electromagnetic problems, [54] for the Stokes system, [40] for the heat equation, [16, 27] for general purposes. On the other hand, the case of a random thickness has been investigated, see [9] in the context of rough surfaces, and [22] for a practical application of approximate boundary conditions to compute moments of solutions of boundary value problems inside random domains. Let us mention the works [4, 18, 43] on polarization tensor for thin inclusions of rough layers.

We restrict here ourselves to layers of uniform thickness. For a review on problems with rapidly oscillating layers, see [44]. See also [26] for an example mixing homogenization and matched asymptotic expansions.

In the case of non-smoooth geometries, the performance of impedance conditions decreases drastically. Nevertheless, they are of very common use in electrical engineering, and are often used for geometries with corners or edges. Users are aware of their limitations, see [37, 49, 46, 7, 53]. In [52], the question of the performance of the impedance condition in the presence of corners has been rigorously investigated. A positive answer is given for the convergence of the approximate problem to the transmission one, as the thickness goes to 0. But it is shown that the performance of the impedance condition is weakened by the presence of corners (the analysis is done for the two-dimensional Laplace equation). To our knowledge, no mathematical work has been done since, which describes a method to overcome this difficulty and recover the convergence rate of the smooth case. The aim of the present paper is to present some improvements in that direction.

2 Outline of the paper

We consider the geometry of Figure 1, where he domain $\Omega_{\rm i}$ corresponds to the material, and $\Omega_{\rm e}^\varepsilon$ the thin layer around a portion of its boundary Γ. The thickness of the layer is small, and we will assume $\varepsilon \leqslant \varepsilon_0$ for some $\varepsilon_0 \geqslant 0$. We look for a solution u^ε such that

$$u^\varepsilon = \begin{cases} u_{\rm i}^\varepsilon & \text{in } \Omega_{\rm i}, \\ u_{\rm e}^\varepsilon & \text{in } \Omega_{\rm e}^\varepsilon, \end{cases}$$

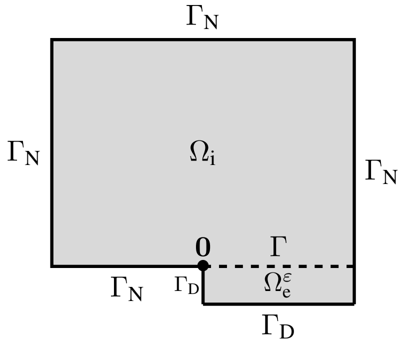

Figure 1: The domain $\Omega^\varepsilon = \Omega_i \cup \Gamma \cup \Omega_e^\varepsilon$.

satisfying the following transmission problem for the Laplace equation

$$\begin{cases} -\alpha\Delta u_i^\varepsilon = f_i & \text{in } \Omega_i, \\ -\Delta u_e^\varepsilon = f_e & \text{in } \Omega_e^\varepsilon, \\ u_i^\varepsilon = u_e^\varepsilon & \text{on } \Gamma, \\ \alpha\partial_\nu u_i^\varepsilon = \partial_\nu u_e^\varepsilon & \text{on } \Gamma, \\ \partial_\nu u_i^\varepsilon = 0 & \text{on } \Gamma_N, \\ u_e^\varepsilon = 0 & \text{on } \Gamma_D. \end{cases} \tag{1}$$

Transmission conditions are set on the inner boundary Γ (dotted line). On the other boundaries Γ_N and Γ_D, homogeneous Neumann and Dirichlet conditions are respectively imposed.

The limit problem ($\varepsilon \to 0$) corresponds to the mixed Neumann-Dirichlet problem. The change of limit condition at the origin implies a lack of regularity of its solution. The splitting into regular and singular parts is possible thanks to the theory of elliptic problems in corner domains, see [39, 33, 24].

In a smooth situation (i.e. no singularity for the limit solution u^0), the following so called *impedance problem* has been introduced, see [28, 11] for example :

$$\begin{cases} -\alpha\Delta v^\varepsilon = f_i & \text{in } \Omega_i, \\ \partial_\nu v^\varepsilon = 0 & \text{on } \Gamma_N, \\ v^\varepsilon + \alpha\varepsilon\partial_\nu v^\varepsilon = 0 & \text{on } \Gamma. \end{cases} \tag{2}$$

This problem is posed in the domain Ω_i (which has no layer, and does not depend on ε).

Following the steps described in [17] for a similar problem with a corner, we explain in Section 3 how to build an asymptotic expansion of its solution u^ε with respect to the small parameter ε. This expansion is then exploited in Section 4 to investigate the accuracy of the standard impedance condition of Robin type (which is valid for smooth situations), i.e. to quantify the error between u_i^ε and v^ε. Sections 5 and 6 are devoted to the description of improvements of the impedance problem (2) in order to obtain a better approximation of the transmission problem (1).

Notation In the following, $L^2(\omega)$ and $H^k(\omega)$ denote the standard Lebesgue and Sobolev spaces in a domain $\omega \subset \mathbb{R}^2$. For $\mathbf{x} \in \mathbb{R}^2$, we set $\mathbf{x} = (x, y)$, and (r, θ) denote the polar coordinates centered at the origin, such that Γ corresponds to $\theta = 0$.

Variational formulations – a priori estimates

- The transmission problem (1) is associated with the following variational formulation

$$\textit{Find } u^\varepsilon \in \mathsf{V}_\mathrm{t} \textit{ such that } \forall \varphi \in \mathsf{V}_\mathrm{t}, \quad \int_{\Omega_\mathrm{i}} \alpha \nabla u_\mathrm{i}^\varepsilon \cdot \nabla \varphi_\mathrm{i} + \int_{\Omega_\mathrm{e}} \nabla u_\mathrm{e}^\varepsilon \cdot \nabla \varphi_\mathrm{e} = \int_{\Omega_\mathrm{i}} f_\mathrm{i} \varphi_\mathrm{i} + \int_{\Omega_\mathrm{e}} f_\mathrm{e} \varphi_\mathrm{e},$$

  where the variational space is given by

$$\mathsf{V}_\mathrm{t} = \{u^\varepsilon \in \mathrm{H}^1(\Omega^\varepsilon)\ ;\ u^\varepsilon = 0 \text{ on } \Gamma_\mathrm{D}\}.$$

  For given L^2-data f_i and f_e, the Lax-Milgram lemma ensures existence and uniqueness of u^ε, together with the *a priori* estimate (with a constant C independent of $\varepsilon \leqslant \varepsilon_0$)

$$\|u^\varepsilon\|_{\mathrm{H}^1(\Omega^\varepsilon)} \leqslant C \left(\|f_\mathrm{i}\|_{\mathrm{L}^2(\Omega_\mathrm{i})} + \|f_\mathrm{e}\|_{\mathrm{L}^2(\Omega_\mathrm{e})} \right).$$

- The Robin problem (2) is associated with the following variational formulation

$$\textit{Find } v^\varepsilon \in \mathsf{V}_\mathrm{r} \textit{ such that } \forall \varphi \in \mathsf{V}_\mathrm{r}, \quad \int_{\Omega_\mathrm{i}} \alpha \nabla v^\varepsilon \cdot \nabla \varphi + \frac{1}{\varepsilon} \int_\Gamma v^\varepsilon \varphi = \int_{\Omega_\mathrm{i}} f_\mathrm{i} \varphi,$$

  where the variational space is given by $\mathsf{V}_\mathrm{r} = \mathrm{H}^1(\Omega_\mathrm{i})$. For a given L^2-datum f_i, the Lax-Milgram lemma ensures existence and uniqueness of v^ε, together with the *a priori* estimate (with a constant again denoted by C independent of $\varepsilon \leqslant \varepsilon_0$)

$$\|v^\varepsilon\|_{\mathrm{H}^1(\Omega_\mathrm{i})} \leqslant C \|f_\mathrm{i}\|_{\mathrm{L}^2(\Omega_\mathrm{i})}.$$

3 Asymptotic expansion of the transmission problem

In a smooth gemetrical framework, thin layer problems are regular perturbation problems. In [11], a complete asymptotic expansion is built in the case where the thin coating lies on the whole boundary of a smooth object. This construction is based on the variational formulation of the problem and leads to suboptimal error estimates, which can be easily improved, see [51, 8].

As already mentioned, in the situation of Figure 1 the limit problem reads

$$\left\{ \begin{array}{rcll} -\alpha \Delta u^0 & = & f_\mathrm{i} & \text{in } \Omega_\mathrm{i}, \\ \partial_\nu u^0 & = & 0 & \text{on } \Gamma_\mathrm{N}, \\ u^0 & = & 0 & \text{on } \Gamma, \end{array} \right. \tag{3}$$

which is singular near the origin due to the change in the boundary conditions at that point. The behavior near $\mathbf{0}$ is precisely described by the theory of corner problems, see [39, 33, 24]:

$$u^0(\mathbf{x}) = u^0_{\text{reg}}(\mathbf{x}) + \gamma \chi(\mathbf{x}) \mathfrak{s}(\mathbf{x}), \tag{4}$$

where $u^0_{\text{reg}} \in \mathrm{H}^2(\Omega_\mathrm{i})$, $\gamma \in \mathbb{R}$ (singular coefficient), $\mathfrak{s}$ (first singular function) is given in polar coordinates by

$$\mathfrak{s}(\mathbf{x}) = \sqrt{r} \sin\left(\frac{\theta}{2}\right),$$

and $\chi \in \mathscr{C}^\infty(\mathbb{R}^2)$ is a smooth radial cutoff function:

$$\chi(\mathbf{x}) = \begin{cases} 1 & \text{if } |\mathbf{x}| < r_0, \\ 0 & \text{if } |\mathbf{x}| > r_1. \end{cases}$$

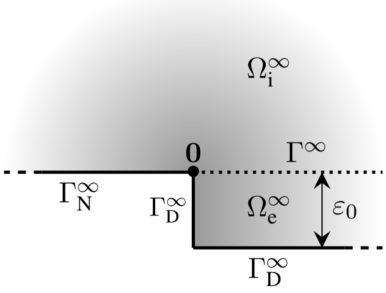

Figure 2: The infinite domain $\Omega^{\infty} = \Omega_{\mathrm{i}}^{\infty} \cup \Gamma^{\infty} \cup \Omega_{\mathrm{e}}^{\infty}$ for the transmission problem.

Compared to the smooth situation, the asymptotic expansion of the solution u^{ε} involves a correction near the corner through a *profile* $\mathfrak{K}$ in the scaled variable $\mathbf{X} = \frac{\mathbf{x}}{\varepsilon}$.

Such a profile satisfies the homogeneous problem with condition at infinity

$$\left\{\begin{array}{rcll} -\alpha\Delta\mathfrak{K}_{\mathrm{i}} &=& 0 & \text{in } \Omega_{\mathrm{i}}^{\infty},\\ -\Delta\mathfrak{K}_{\mathrm{e}} &=& 0 & \text{in } \Omega_{\mathrm{e}}^{\infty},\\ \mathfrak{K}_{\mathrm{i}} &=& \mathfrak{K}_{\mathrm{e}} & \text{on } \Gamma^{\infty},\\ \alpha\partial_{\nu}\mathfrak{K}_{\mathrm{i}} &=& \partial_{\nu}\mathfrak{K}_{\mathrm{e}} & \text{on } \Gamma^{\infty},\\ \partial_{\nu}\mathfrak{K}_{\mathrm{i}} &=& 0 & \text{on } \Gamma_{\mathrm{N}}^{\infty},\\ \mathfrak{K}_{\mathrm{e}} &=& 0 & \text{on } \Gamma_{\mathrm{D}}^{\infty},\\ \mathfrak{K} &=& \mathfrak{s} + o\big(\sqrt{|\mathbf{X}|}\big) & \text{at infinity,} \end{array}\right. \tag{5}$$

in the infinite domain of Figure 2 ($\mathfrak{s}$ is extended by 0 in $\Omega_{\mathrm{e}}^{\infty}$ for the condition at infinity).

It is not straightforward that the profile $\mathfrak{K}$ involved in the asymptotic expansion is well-defined by Problem (5). We also need to know precisely the behavior of $\mathfrak{K}$ at infinity. The useful results are summarized below.

Proposition 1 (Existence and behavior at infinity for the transmission profile) *Problem* (5) *has a unique solution. The profile $\mathfrak{K}$ admits the following behavior at infinity in $\Omega_{\mathrm{i}}^{\infty}$*

$$\mathfrak{K}_{\mathrm{i}}(\mathbf{X}) = \mathfrak{s}(\mathbf{X}) + \mathfrak{l}(\mathbf{X}) + \mu\,\mathfrak{s}^{\star}(\mathbf{X}) + \mathcal{O}\left(|\mathbf{X}|^{-\frac{3}{2}}\log^2|\mathbf{X}|\right), \tag{6}$$

where

- $\mathfrak{l}(\mathbf{X}) = \dfrac{\alpha}{2\pi\sqrt{|\mathbf{X}|}}\left((\pi-\theta)\cos\frac{\theta}{2} + \log|\mathbf{X}|\sin\frac{\theta}{2}\right)$,
- $\mathfrak{s}^{\star}(\mathbf{X}) = \dfrac{1}{\sqrt{|\mathbf{X}|}}\sin\frac{\theta}{2}$.

The function $\mathfrak{s}^{\star}$ is called dual singular function. *The number $\mu \in \mathbb{R}$ is characteristic of the geometry and the operator (it depends on the transmission coefficient α).*

Proof: The existence is based on the weighted variational space

$$\mathfrak{V} = \left\{\mathfrak{v} \in \mathrm{H}^1_{\mathrm{loc}}(\Omega^{\infty})) \ ; \ \nabla\mathfrak{v} \in \mathrm{L}^2(\Omega^{\infty}) \text{ and } \mathfrak{v} = 0 \text{ on } \Gamma_{\mathrm{D}}^{\infty}\right\},$$

and the behavior at infinity relies on the Laplace-Mellin transform, see [51]. ■

The expansion of the solution of the transmission problem can be detailed using the profile $\mathfrak{K}$, emphasizing the dependence in the parameters γ (singular coefficients in the splitting (4) of the limit solution u_0), and μ (coefficient of the dual singular function in the behavior at infinity (6) of the profile $\mathfrak{K}$).

Proposition 2 (Asymptotic expansion for the transmission problem) *The solution u^ε of the transmission problem* (1) *admits the following asymptotics as $\varepsilon \to 0$*

$$u_{\mathrm{i}}^\varepsilon(\mathbf{x}) = u^0(\mathbf{x}) + \gamma\chi(\mathbf{x})\sqrt{\varepsilon}(\mathfrak{K}_{\mathrm{i}} - \mathfrak{s})\left(\tfrac{\mathbf{x}}{\varepsilon}\right) + \gamma\varepsilon u_{1,0}(\mathbf{x}) + \gamma\mu\varepsilon u_{1,1}(\mathbf{x}) + \varepsilon u_1(\mathbf{x})$$
$$+\gamma\varepsilon\log\varepsilon\, u_{1,2}(\mathbf{x}) + \mathcal{O}_{\mathrm{H}^1(\Omega_{\mathrm{i}})}\left(\varepsilon^{\frac{3}{2}}\log^2\varepsilon\right),$$

$$u_{\mathrm{e}}^\varepsilon(\mathbf{x}) = \gamma\chi(\mathbf{x})\sqrt{\varepsilon}\,\mathfrak{K}_{\mathrm{e}}\left(\tfrac{\mathbf{x}}{\varepsilon}\right) - \varepsilon\alpha\left(\tfrac{y}{\varepsilon}+1\right)\partial_\nu u^0_{\mathrm{reg}}\big|_\Gamma(x) + \mathcal{O}_{\mathrm{H}^1(\Omega_{\mathrm{e}}^\varepsilon)}\left(\varepsilon^{\frac{3}{2}}\log^2\varepsilon\right),$$

where the terms $u_{1,j}$ and u_1 are defined by problems (8) *and* (10) *below respectively.*

Proof: Let us describe the construction of the first terms in the asymptotic expansion. The first remainder after correction is defined by

$$r_0^\varepsilon(\mathbf{x}) = \begin{cases} u^\varepsilon(\mathbf{x}) - u^0(\mathbf{x}) - \gamma\chi(\mathbf{x})\sqrt{\varepsilon}(\mathfrak{K}_{\mathrm{i}} - \mathfrak{s})\left(\tfrac{\mathbf{x}}{\varepsilon}\right) & \text{in } \Omega_{\mathrm{i}}, \\ u^\varepsilon(\mathbf{x}) - \gamma\chi(\mathbf{x})\sqrt{\varepsilon}\,\mathfrak{K}_{\mathrm{e}}\left(\tfrac{\mathbf{x}}{\varepsilon}\right) & \text{in } \Omega_{\mathrm{e}}^\varepsilon. \end{cases}$$

It solves the following transmission problem

$$\begin{cases} -\alpha\Delta r_{0,\mathrm{i}}^\varepsilon = f_{\mathrm{i}}^\varepsilon & \text{in } \Omega_{\mathrm{i}}, \\ -\Delta r_{0,\mathrm{e}}^\varepsilon = f_{\mathrm{e}}^\varepsilon & \text{in } \Omega_{\mathrm{e}}^\varepsilon, \\ r_{0,\mathrm{i}}^\varepsilon = r_{0,\mathrm{e}}^\varepsilon & \text{on } \Gamma, \\ \alpha\partial_\nu r_{0,\mathrm{i}}^\varepsilon = \partial_\nu r_{0,\mathrm{e}}^\varepsilon - \alpha\partial_\nu u^0_{\mathrm{reg}} & \text{on } \Gamma, \\ \partial_\nu r_{0,\mathrm{i}}^\varepsilon = 0 & \text{on } \Gamma_{\mathrm{N}}, \\ r_{0,\mathrm{e}}^\varepsilon = 0 & \text{on } \Gamma_{\mathrm{D}}, \end{cases} \tag{7}$$

with

$$f_{\mathrm{i}}^\varepsilon(\mathbf{x}) = -\alpha\gamma\sqrt{\varepsilon}\left(\Delta\chi(\mathbf{x})(\mathfrak{K}_{\mathrm{i}} - \mathfrak{s})\left(\tfrac{\mathbf{x}}{\varepsilon}\right) + \frac{2}{\varepsilon}\nabla\chi(\mathbf{x})\cdot\nabla(\mathfrak{K}_{\mathrm{i}} - \mathfrak{s})\left(\tfrac{\mathbf{x}}{\varepsilon}\right)\right),$$

$$f_{\mathrm{e}}^\varepsilon(\mathbf{x}) = -\gamma\sqrt{\varepsilon}\left(\Delta\chi(\mathbf{x})\mathfrak{K}_{\mathrm{e}}\left(\tfrac{\mathbf{x}}{\varepsilon}\right) + \frac{2}{\varepsilon}\nabla\chi(\mathbf{x})\cdot\nabla\mathfrak{K}_{\mathrm{e}}\left(\tfrac{\mathbf{x}}{\varepsilon}\right)\right).$$

Since both $\Delta\chi(\mathbf{x})$ and $\nabla\chi(\mathbf{x})$ vanish for $|\mathbf{x}| < r_0$, we may exploit the behavior of $\mathfrak{K}$ at infinity to obtain an expansion of f^ε with respect to ε. Indeed, using (6), we obtain for $|\mathbf{x}| > r_0$,

$$(\mathfrak{K}_{\mathrm{i}} - \mathfrak{s})\left(\tfrac{\mathbf{x}}{\varepsilon}\right) = \sqrt{\varepsilon}\,\phi_0(\mathbf{x}) + \mu\sqrt{\varepsilon}\,\mathfrak{s}^\star(\mathbf{x}) + \sqrt{\varepsilon}\log\varepsilon\,\phi_2(\mathbf{x}) + \mathcal{O}_{\mathrm{L}^\infty(\Omega_{\mathrm{i}})}\left(\varepsilon^{\frac{3}{2}}\log^2\varepsilon\right),$$

for some explicit functions ϕ_0 and ϕ_2. Similarly for the gradients, we get

$$\nabla(\mathfrak{K}_{\mathrm{i}} - \mathfrak{s})\left(\tfrac{\mathbf{x}}{\varepsilon}\right) = \varepsilon^{\frac{3}{2}}\,\mathbf{F}_0(\mathbf{x}) + \mu\varepsilon^{\frac{3}{2}}\,\mathbf{F}_1(\mathbf{x}) + \varepsilon^{\frac{3}{2}}\log\varepsilon\,\mathbf{F}_2(\mathbf{x}) + \mathcal{O}_{\mathrm{L}^\infty(\Omega_{\mathrm{i}})}\left(\varepsilon^{\frac{5}{2}}\log^2\varepsilon\right),$$

for some (explicit) vector functions $\mathbf{F}_0$, $\mathbf{F}_1$, and $\mathbf{F}_2$. This leads to the expansion

$$f_{\mathrm{i}}^\varepsilon(\mathbf{x}) = \alpha\gamma\sqrt{\varepsilon}\left(\sqrt{\varepsilon}\,f_0(\mathbf{x}) + \sqrt{\varepsilon}\log\varepsilon\,f_1(\mathbf{x}) + \mu\sqrt{\varepsilon}\,f_2(\mathbf{x})\right) + \mathcal{O}_{\mathrm{L}^\infty(\Omega_{\mathrm{i}})}\left(\varepsilon^2\log^2\varepsilon\right),$$

where the functions f_1, f_2, f_3 can be explicitly expressed thanks to the ϕ_j and the $\mathbf{F}_j$. We naturally define the corrector terms $u_{1,j}$ ($j = 0, 1, 2$) as solutions to the problems

$$\left\{\begin{array}{rcll} -\alpha\Delta u_{1,j} &=& f_j & \text{in } \Omega_{\rm i}, \\ u_{1,j} &=& 0 & \text{on } \Gamma, \\ \partial_\nu u_{1,j} &=& 0 & \text{on } \Gamma_{\rm N}. \end{array}\right. \tag{8}$$

For the exterior part, a dilation in the vertical direction y is performed in the thin layer. Setting

$$Y = \tfrac{y}{\varepsilon}\varepsilon_0,$$

(for some fixed $\varepsilon_0 > 0$), the operators Δ and ∂_ν become $\frac{\varepsilon_0^2}{\varepsilon^2}\partial_Y^2 + \partial_x^2$ and $\frac{\varepsilon_0}{\varepsilon}\partial_Y$, respectively. Thus, the first correcting term has the form $\varepsilon U_1(x, \frac{y}{\varepsilon}\varepsilon_0)$ where U_1 solves

$$\left\{\begin{array}{rcll} -\partial_Y^2 U_1 &=& 0 & \text{for } Y \in (0,1), \\ \partial_Y U_1 &=& -\frac{\alpha}{\varepsilon_0}\partial_\nu u^0_{\rm reg} & \text{for } Y = 0, \\ U_1 &=& 0 & \text{for } Y = -\varepsilon_0, \end{array}\right. \tag{9}$$

leading to

$$U_1(x, Y) = -(\tfrac{Y}{\varepsilon_0} + 1)\alpha\partial_\nu u^0_{\rm reg}\big|_\Gamma(x).$$

The term $\varepsilon U_1(x, \frac{y}{\varepsilon})$ implies a contribution in the interior domain as well, denoted by u_1, solution to

$$\left\{\begin{array}{rcll} -\alpha\Delta u_1 &=& 0 & \text{in } \Omega_{\rm i}, \\ u_1 &=& -\alpha\partial_\nu u^0_{\rm reg} & \text{on } \Gamma, \\ \partial_\nu u_1 &=& 0 & \text{on } \Gamma_{\rm N}. \end{array}\right. \tag{10}$$

Note that the contribution of $f^\varepsilon_{\rm e}$ will be of higher order since Δ is an operator $\mathcal{O}(\varepsilon^{-2})$ in variables (x, Y).

To obtain error estimates, we need to build the asymptotic expansion further since the *a priori* estimates are not sharp enough. This is a classical procedure for the proofs of convergence in the sense of asymptotic expansions. We refer to [17] for more details. ■

4 Accuracy of the impedance condition

The impedance problem with Robin boundary condition admits a similar asymptotic expansion, whose construction has been sketched in [21]. A profile $\mathfrak{z}$ has to be introduced, solving the homogeneous problem with condition at infinity

$$\left\{\begin{array}{rcll} -\alpha\Delta\mathfrak{z} &=& 0 & \text{in } \Omega_{\rm i}^\infty, \\ \mathfrak{z} + \alpha\partial_\nu\mathfrak{z} &=& 0 & \text{on } \Gamma^\infty, \\ \partial_\nu\mathfrak{z} &=& 0 & \text{on } \Gamma_{\rm N}^\infty, \\ \mathfrak{z} &=& \mathfrak{s} + o(\sqrt{|\mathbf{X}|}) & \text{at infinity}, \end{array}\right. \tag{11}$$

in the infinite domain of Figure 3.

The profile $\mathfrak{z}$ admits a similar behavior at infinity than $\mathfrak{K}$, with another coefficient in front of the dual singularity $\mathfrak{s}^\star$.

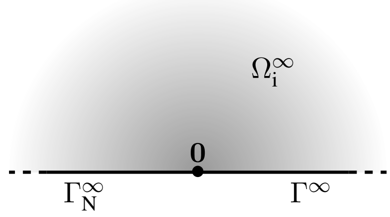

Figure 3: The infinite domain for the impedance problem.

Proposition 3 (Existence and behavior at infinity for the impedance profile) *Problem* (11) *has a unique solution. The profile* $\mathfrak{z}$ *admits the following behavior at infinity in* $\Omega_{\mathrm{i}}^{\infty}$

$$\mathfrak{z}(\mathbf{X}) = \mathfrak{s}(\mathbf{X}) + \mathfrak{l}(\mathbf{X}) + \lambda\,\mathfrak{s}^{\star}(\mathbf{X}) + \mathcal{O}\left(|\mathbf{X}|^{-\frac{3}{2}}\log^2|\mathbf{X}|\right). \tag{12}$$

The number $\lambda \in \mathbb{R}$ *is characteristic of the geometry and the operator (it depends on the impedance coefficient* α*).*

Proposition 4 (Asymptotic expansion for the impedance problem) *The solution* v^{ε} *of the impedance problem* (2) *admits the following asymptotics*

$$v^{\varepsilon}(\mathbf{x}) = u^0(\mathbf{x}) + \gamma\chi(\mathbf{x})\sqrt{\varepsilon}(\mathfrak{z}-\mathfrak{s})\left(\tfrac{\mathbf{x}}{\varepsilon}\right) + \varepsilon u_{1,0}(\mathbf{x}) + \gamma\lambda\varepsilon u_{1,1}(\mathbf{x}) + \varepsilon u_1(\mathbf{x})$$
$$+\varepsilon\log\varepsilon\, u_{1,2}(\mathbf{x}) + \mathcal{O}_{\mathrm{H}^1(\Omega_{\mathrm{i}})}\left(\varepsilon^{\frac{3}{2}}\log^2\varepsilon\right),$$

Proof: The proof is very similar to the proof of Proposition 2. Instead of expanding the term $(\mathfrak{K}-\mathfrak{s})\left(\frac{\mathbf{x}}{\varepsilon}\right)$, we need to expand $(\mathfrak{z}-\mathfrak{s})\left(\frac{\mathbf{x}}{\varepsilon}\right)$. In the behavior at infinity of the profile $\mathfrak{z}$, the only difference (up to the remainder in $\mathbf{X}|^{-\frac{3}{2}}\log^2|\mathbf{X}|$) is the coefficient λ, which generically differs from the coefficient μ. Thus, the f_j remain unchanged, and the same terms $u_{1,j}$ are to be defined. Concerning the term u_1, it coincides with its counterpart for the Robin problem by construction of the impedance condition. ■

Propositions 2 and 4 make it possible to compare the solutions of the transmission and impedance problems.

Theorem 5 (Accuracy of the impedance approximation) *The solutions* u^{ε} *and* v^{ε} *of Problems* (1) *and* (2) *satisfy*

$$u_{\mathrm{i}}^{\varepsilon} - v^{\varepsilon} = \gamma\sqrt{\varepsilon}\,(\mathfrak{K}-\mathfrak{z})\left(\tfrac{\mathbf{x}}{\varepsilon}\right) + \varepsilon\gamma(\mu-\lambda)u_{1,1}(\mathbf{x}) + \mathcal{O}_{\mathrm{H}^1(\Omega_{\mathrm{i}})}\left(\varepsilon^{\frac{3}{2}}\log^2\varepsilon\right), \tag{13}$$

with

- $\|\sqrt{\varepsilon}\,(\mathfrak{K}-\mathfrak{z})\left(\tfrac{\cdot}{\varepsilon}\right)\|_{\mathrm{H}^1(\Omega_{\mathrm{i}})} = \mathcal{O}(\sqrt{\varepsilon})$,
- $\|\sqrt{\varepsilon}\,(\mathfrak{K}-\mathfrak{z})\left(\tfrac{\cdot}{\varepsilon}\right)\|_{\mathrm{L}^2(\Omega_{\mathrm{i}})} = |\mu-\lambda|\mathcal{O}(\varepsilon) + \mathcal{O}(\varepsilon^{\frac{3}{2}})$.

This leads to the the following error estimates

$$\|u_{\mathrm{i}}^{\varepsilon} - v^{\varepsilon}\|_{\mathrm{H}^1(\Omega_{\mathrm{i}})} = \mathcal{O}(\sqrt{\varepsilon}), \qquad \|u_{\mathrm{i}}^{\varepsilon} - v^{\varepsilon}\|_{\mathrm{L}^2(\Omega_{\mathrm{i}})} = \mathcal{O}(\varepsilon).$$

Let us emphasize that, in the *smooth* case (i.e. where the layer $\Omega_{\mathrm{e}}^{\varepsilon}$ lies on the whole bottom edge of the square Ω_{i}), the error estimate is $\mathcal{O}(\varepsilon^3)$ for both L^2 and H^1 norms. The precision of the impedance condition is harshly decreased in the present situation. Numerical evidence is given in [52] for corner domains.

5 Improved impedance conditions

In this section, we present two modifications of the impedance condition to improve the L^2-error estimate.

5.1 Multiscale Robin-type impedance condition

Instead of setting the standard impedance condition $v^\varepsilon + \alpha\varepsilon\partial_\nu v^\varepsilon = 0$ on Γ, we propose the following impedance problem of Robin type with a variable coefficient of the form

$$\left\{\begin{array}{rcll} -\alpha\Delta v_\bullet^\varepsilon &=& f_\mathrm{i} & \text{in } \Omega_\mathrm{i}, \\ \partial_\nu v_\bullet^\varepsilon &=& 0 & \text{on } \Gamma_\mathrm{N}, \\ v_\bullet^\varepsilon + \varepsilon\alpha_\bullet\left(\frac{\cdot}{\varepsilon}\right)\partial_\nu v_\bullet^\varepsilon &=& 0 & \text{on } \Gamma, \end{array}\right. \tag{14}$$

where $\alpha_\bullet$ is a piecewise linear function coinciding with the constant α far from the origin, see Figure 4. We seek a value of the parameter $\rho_\bullet$ so that the error $\|u_\mathrm{i}^\varepsilon - v_\bullet^\varepsilon\|_{\mathrm{L}^2(\Omega_\mathrm{i})}$ is of smaller order than $\|u_\mathrm{i}^\varepsilon - v^\varepsilon\|_{\mathrm{L}^2(\Omega_\mathrm{i})}$ as $\varepsilon \to 0$.

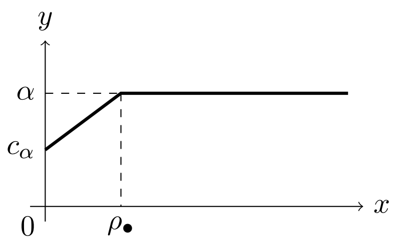

Figure 4: The function $x \mapsto \alpha_\bullet(x)$.

5.1.1 Theoretical justification

The technique used for the classical impedance problem can be used for Problem (14) to obtain the asymptotic expansion of $v_\bullet^\varepsilon$. Similarly, a profile needs to be introduced, solving an homogeneous problem in the infinite domain Ω_i^∞:

$$\left\{\begin{array}{rcll} -\alpha\Delta\mathfrak{z}_\bullet &=& 0 & \text{in } \Omega_\mathrm{i}^\infty, \\ \mathfrak{z}_\bullet + \alpha_\bullet\partial_\nu\mathfrak{z}_\bullet &=& 0 & \text{on } \Gamma^\infty, \\ \partial_\nu\mathfrak{z}_\bullet &=& 0 & \text{on } \Gamma_\mathrm{N}^\infty, \\ \mathfrak{z}_\bullet &=& \mathfrak{s} + o(\sqrt{r}) & \text{at infinity.} \end{array}\right. \tag{15}$$

The profile $\mathfrak{z}_\bullet$ admits a similar behavior at infinity than $\mathfrak{K}$ and $\mathfrak{z}$:

Proposition 6 (Existence and behavior at infinity for the modified Robin impedance profile) *Problem* (15) *has a unique solution. The profile $\mathfrak{z}_\bullet$ admits the following behavior at infinity in Ω_i^∞*

$$\mathfrak{z}_\bullet(\mathbf{X}) = \mathfrak{s}(\mathbf{X}) + \mathfrak{l}(\mathbf{X}) + \lambda_\bullet\,\mathfrak{s}^\star(\mathbf{X}) + \mathcal{O}\left(|\mathbf{X}|^{-\frac{3}{2}}\log^2(|\mathbf{X}|)\right). \tag{16}$$

The number $\lambda_\bullet \in \mathbb{R}$ depends in particular on the parameter $\rho_\bullet$.

In the asymptotic expansion of $v_\bullet^\varepsilon$, the only difference with respect to v^ε concerns the profile $\mathfrak{z}_\bullet$ and its principal characteristic coefficient at infinity $\lambda_\bullet$.

Proposition 7 (Asymptotic expansion for the impedance problem) *The solution $v_\bullet^\varepsilon$ of the modified Robin impedance problem* (14) *admits the following asymptotics*

$$v_\bullet^\varepsilon(\mathbf{x}) = u^0(\mathbf{x}) + \gamma\chi(\mathbf{x})\sqrt{\varepsilon}(\mathfrak{z}_\bullet - \mathfrak{s})\left(\tfrac{\mathbf{x}}{\varepsilon}\right) + \varepsilon u_{1,0}(\mathbf{x}) + \gamma\lambda_\bullet \varepsilon u_{1,1}(\mathbf{x}) + \varepsilon u_1(\mathbf{x})$$
$$+\varepsilon \log\varepsilon\, u_{1,2}(\mathbf{x}) + \mathcal{O}_{\mathrm{H}^1(\Omega_\mathrm{i})}\left(\varepsilon^{\frac{3}{2}}\log^2\varepsilon\right).$$

Theorem 5 is merely adapted and we obtain

$$u_\mathrm{i}^\varepsilon - v_\bullet^\varepsilon = \gamma\sqrt{\varepsilon}\,(\mathfrak{K} - \mathfrak{z}_\bullet)\left(\tfrac{\mathbf{x}}{\varepsilon}\right) + \varepsilon\gamma(\mu - \lambda_\bullet)u_{1,1}(\mathbf{x}) + \mathcal{O}_{\mathrm{H}^1(\Omega_\mathrm{i})}\left(\varepsilon^{\frac{3}{2}}\log^2\varepsilon\right). \tag{17}$$

Actually, it is possible to choose $\rho_\bullet$ such that $\lambda_\bullet = \mu$, and thus improve the L^2-error.

Theorem 8 (Error estimate for the modified Robin impedance condition) *There exists $\rho_\bullet > 0$ such that $\lambda_\bullet = \mu$. For this value of $\rho_\bullet$, we have*

$$\|u_\mathrm{i}^\varepsilon - v_\bullet^\varepsilon\|_{\mathrm{L}^2(\Omega_\mathrm{i})} = \mathcal{O}\left(\varepsilon^{\frac{3}{2}}\log^2\varepsilon\right).$$

Proof: We consider the following problem in the bounded domain Ω^R obtained by intersecting Ω_i^∞ with the ball of radius R, and Ω_e^∞ with $[x < R]$, see Figure 5.

$$\begin{cases} -\alpha\Delta\mathfrak{K}_\mathrm{i}^R &= 0 & \text{in } \Omega_\mathrm{i}^R, \\ -\Delta\mathfrak{K}_\mathrm{e}^R &= 0 & \text{in } \Omega_\mathrm{e}^R, \\ \mathfrak{K}_\mathrm{i}^R &= \mathfrak{K}_\mathrm{e}^R & \text{on } \Gamma^R, \\ \alpha\partial_\nu\mathfrak{K}_\mathrm{i}^R &= \partial_\nu\mathfrak{K}_\mathrm{e}^R & \text{on } \Gamma^R, \\ \partial_\nu\mathfrak{K}_\mathrm{i}^R &= 0 & \text{on } \Gamma_\mathrm{N}^R, \\ \mathfrak{K}_\mathrm{e}^R &= 0 & \text{on } \Gamma_\mathrm{D}^R, \\ \partial_\nu\mathfrak{K}^R &= \partial_\nu\mathfrak{s} & \text{on } \Gamma_\mathrm{a}^R, \end{cases} \tag{18}$$

Note that the condition on Γ_a^R is an artificial boundary condition, which ensures that $\mathfrak{K}^R \to \mathfrak{K}$ as $R \to +\infty$.

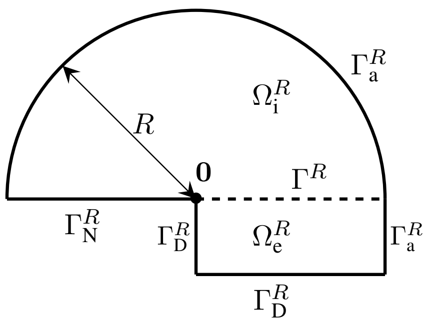

Figure 5: The bounded domain $\Omega^R = \Omega_\mathrm{i}^R \cup \Gamma^R \cup \Omega_\mathrm{e}^R$.

The same can be done for the multiscale Robin problem (15), leading to

$$\begin{cases} -\alpha\Delta\mathfrak{z}_\bullet^R &= 0 & \text{in } \Omega_\mathrm{i}^R, \\ \mathfrak{z}_\bullet^R + \alpha_\bullet\partial_\nu\mathfrak{z}_\bullet^R &= 0 & \text{on } \Gamma^R, \\ \partial_\nu\mathfrak{z}_\bullet^R &= 0 & \text{on } \Gamma_\mathrm{N}^R, \\ \partial_\nu\mathfrak{z}_\bullet^R &= \partial_\nu\mathfrak{s} & \text{on } \Gamma_\mathrm{a}^R. \end{cases} \tag{19}$$

Again, we have $\mathfrak{z}_\bullet^R \to \mathfrak{z}_\bullet$ as $R \to \infty$. The coefficients μ and $\lambda_\bullet$ can be approximated by integrals of $\mathfrak{K}^R$ and $\mathfrak{z}_\bullet^R$ on the circular part of the artificial boundary Γ_{a}^R:

$$I_\bullet(R) = \frac{2}{\pi}\int_0^\pi \Big[\mathfrak{z}_\bullet^R(R,\theta) - \mathfrak{s}(R,\theta) - \mathfrak{l}(R,\theta)\Big]\mathfrak{s}^\star(R,\theta)\,\mathrm{d}\theta,$$

$$I(R) = \frac{2}{\pi}\int_0^\pi \Big[\mathfrak{K}_{\mathrm{i}}^R(R,\theta) - \mathfrak{s}(R,\theta) - \mathfrak{l}(R,\theta)\Big]\mathfrak{s}^\star(R,\theta)\,\mathrm{d}\theta.$$

We will show the existence of $\rho_\bullet(R)$ such that $I_\bullet(R) = I(R)$. Thanks to Lemma 9 below, the mapping $\rho_\bullet \mapsto I_\bullet(R)$ is continuous. It remains to see that $I(R)$ does belong to its range. A sufficient condition for this is the following

$$\textit{for } \rho_\bullet = 0,\ I_\bullet(R) \geqslant I(R), \quad \textit{and for } \rho_\bullet \text{ large enough},\ I_\bullet \leqslant I(R),$$

which is satisfied for an appropriate choice of c_α, see Lemma 10 and 11 below.

The obtained parameter $\rho_\bullet(R)$ ensuring $I_\bullet(R) = I(R)$ obviously depends on the radius R. It can be seen that $\rho_\bullet(R)$ is bounded and we can assume – up to a subsequence – that it converges to some $\rho_\bullet$ as R goes to infinity. The uniform convergence of the integrals $I_\bullet(R)$ with respect to $\rho_\bullet$ as $R \to +\infty$ allows to conclude that $\lambda_\bullet = \mu$ for the obtained value $\rho_\bullet$.

Relying on equation (17), where $\mu = \lambda_\bullet$, we obtain (compare with Theorem 5)

$$\|u_{\mathrm{i}}^\varepsilon - v_\bullet^\varepsilon\|_{\mathrm{L}^2(\Omega_{\mathrm{i}})} = \mathcal{O}\left(\varepsilon^{\frac{3}{2}}\log^2\varepsilon\right).$$

■

lemma 9 *The mapping $\rho_\bullet \mapsto I_\bullet(R)$ is continuous and decreasing.*

Proof: We can apply a maximum principle to problem (19) – for general maximum principles with Robin-type conditions, see [41]. Since the function g is nonnegative, the solution $\mathfrak{z}_\bullet^R$ is nonnegative in Ω_{i}^R.

For $\rho_\bullet$ et $\rho_\circ$ two given positive real numbers, the difference $p^R = \mathfrak{z}_\bullet^R - \mathfrak{z}_\circ^R$ solves the problem

$$\left\{\begin{array}{rcll} -\alpha\Delta p^R &=& 0 & \text{in } \Omega_{\mathrm{i}}^R,\\ p^R + \alpha_\bullet\partial_\nu p^R &=& -(\alpha_\bullet - \alpha_\circ)\partial_\nu \mathfrak{z}_\bullet^R & \text{on } \Gamma^R,\\ \partial_\nu p^R &=& 0 & \text{on } \Gamma_{\mathrm{N}}^R,\\ \frac{1}{2R}p^R + \partial_\nu p^R &=& 0 & \text{on } \Gamma_{\mathrm{a}}^R. \end{array}\right. \tag{20}$$

But $\mathfrak{z}_\bullet^R = -\alpha_\bullet\partial_\nu\mathfrak{z}_\bullet^R$ on Γ^R, which implies $\partial_\nu\mathfrak{z}_\bullet^R \leqslant 0$ on Γ^R. Thus, if $\alpha_\bullet \geqslant \alpha_\circ$, the datum in Problem (20) is nonnegative, and so is its solution. We have obtained $\mathfrak{z}_\bullet^R \geqslant \mathfrak{z}_\circ^R$ for $\alpha_\bullet \geqslant \alpha_\circ$, which implies that $\rho_\bullet \mapsto I_\bullet(R)$ is decreasing.

A standard *a priori* estimate on Problem (20) (via the Poincaré-Friedrichs inequality) gives

$$\|p\|_{\mathrm{H}^1(\Omega_{\mathrm{i}})} \leqslant C\|\alpha_\bullet - \alpha_\circ\|_{\mathrm{L}^\infty(\Gamma^R)},$$

with a positive constant C, which ensures the continuity. ■

lemma 10 *For $\rho_\bullet = 0$, we have $I_\bullet(R) \geqslant I(R)$.*

Proof: For $\rho_\bullet = 0$, the boundary condition on Γ^R is nothing but the classical impedance condition. We will build an extension of $\mathfrak{z}_\bullet^R$ to Ω^R to be able to use a comparison principle with $\mathfrak{K}_\mathrm{i}$. To this end, we set for $\mathbf{x} \in \Omega_\mathrm{e}^R$,

$$\mathfrak{z}_{\bullet,\mathrm{e}}^R(x,y) = (1+y)\mathfrak{z}_\bullet^R(x,0) - cy^2, \tag{21}$$

with a constant c to be adjusted. Obviously, for $y=0$, we get

$$\mathfrak{z}_{\bullet,\mathrm{e}}^R(x,0) = \mathfrak{z}_\bullet^R(x,0) \quad \text{and} \quad \partial_y \mathfrak{z}_\bullet^R(x,0) = \mathfrak{z}_\bullet^R(x,0) = -\alpha\partial_\nu \mathfrak{z}_\bullet^R(x,0),$$

which are the natural transmission conditions across Γ^R. Setting $\mathfrak{q} = \mathfrak{z}_\bullet^R - \mathfrak{K}^R$, the function $\mathfrak{q}$ solves the following transmission condition

$$\begin{cases} -\alpha\Delta\mathfrak{q}_\mathrm{i} &= 0 & \text{in } \Omega_\mathrm{i}^R, \\ -\Delta\mathfrak{q}_\mathrm{e} &= \mathfrak{f}_\mathrm{e} & \text{in } \Omega_\mathrm{e}^R, \\ \mathfrak{q}_\mathrm{i} &= \mathfrak{q}_\mathrm{e} & \text{on } \Gamma^R, \\ \alpha\partial_\nu\mathfrak{q}_\mathrm{i} &= \partial_\nu\mathfrak{q}_\mathrm{e} & \text{on } \Gamma^R, \\ \partial_\nu\mathfrak{q} &= 0 & \text{on } \Gamma_\mathrm{N}^R, \\ \mathfrak{q}_\mathrm{e} &= \mathfrak{h} & \text{on } \Gamma_\mathrm{D}^R, \\ \frac{1}{2R}\mathfrak{q} + \partial_\nu\mathfrak{q} &= 0 & \text{on } \Gamma_\mathrm{a}^R, \end{cases}$$

with

- $\mathfrak{f}_\mathrm{e}(x,y) = -(1+y)\partial_y^2\mathfrak{z}_\bullet^R(x,0) + 2c$,
- $\mathfrak{h}(x,y) = (1+y)\mathfrak{z}_\bullet^R(x,0) - cy^2$.

If $\mathfrak{f}_\mathrm{e} \geqslant 0$ and $\mathfrak{h} \geqslant 0$, then we are able to conclude that $\mathfrak{q} \geqslant 0$, which gives the stated result. Under the assumption that $\partial_x^2\mathfrak{z}_\bullet^R$ is bounded on Γ^R (which is actually false, see below), we can choose $c \geqslant \frac{1}{2}\max_x \partial_x^2\mathfrak{z}_\bullet^R(x,0)$ so that $\mathfrak{f}_\mathrm{e} \geqslant 0$. For such a choice of c, it is possible to ensure $\mathfrak{h} \geqslant 0$ provided ε_0 is sufficiently small.

The previous argumentation is not correct since $\partial_x^2\mathfrak{z}_\bullet^R \to +\infty$ as $x \to 0$ (a detailed analysis of the Robin singularities shows that $\mathfrak{z}_\bullet^R(x,0) \sim kx\log x$, $\partial_x\mathfrak{z}_\bullet^R(x,0) \sim k\log x$, and $\partial_x^2\mathfrak{z}_\bullet^R(x,0) \sim kx^{-1}$ with a positive constant k). To overcome this difficulty, we remark that $\mathfrak{K}^R(0,0) = 0$ and $\mathfrak{z}_\bullet^R(0,0) > 0$ (clearly, $\mathfrak{z}_\bullet^R(0,0) \geqslant 0$ by a maximum principle, and since its derivative with respect to x is $-\infty$ at $(0,0)$, the value of $\mathfrak{z}_\bullet^R$ is positive at the origin). We can then introduce $\eta > 0$ such that $\mathfrak{z}_\bullet^R(x,0) \geqslant \mathfrak{K}_\mathrm{e}^R(x,y)$ for $0 < x < \eta$ and $-\varepsilon_0 < y < 0$ (note that this value of η depends on ε_0, but stil holds for smaller values of ε_0).

We consider the domain $\Omega^{R,\eta}$ where the layer only lies on the part $x > \eta$ of Γ^R, see Figure 6. By definition of η, the function $\mathfrak{q} = \mathfrak{z}_\bullet^R - \mathfrak{K}^R$ is nonnegative on the dotted part of $\Gamma_\mathrm{D}^{R,\eta}$. The previous extension in the layer becomes possible since $\partial_x^2\mathfrak{z}_\bullet^R$ is bounded on $\Gamma^{R,\eta}$. The constants c and ε_0 can be adjusted (without any influence on η) so that we can apply the maximum principle and obtain $\mathfrak{q} \geqslant 0$. ■

lemma 11 *There exists $\rho_\bullet > 0$ and $c_\alpha > 0$, such that $I_\bullet(R) \leqslant I(R)$.*

Proof: If $\rho_\bullet \to \infty$, then the function $\alpha_\bullet$ tends to the constant c_α. The boundary condition on Γ^R is then $\mathfrak{z}_\bullet^R + c_\alpha\partial_\nu\mathfrak{z}_\bullet^R = 0$. If $c_\alpha \to 0$, then the function $\mathfrak{z}_\bullet^R$ converges (in the L^∞-sense) to the

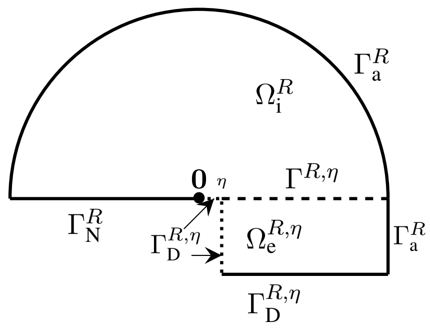

Figure 6: The perturbed domain $\Omega^{R,\eta} = \Omega_{\rm i}^R \cup \Gamma^{R,\eta} \cup \Omega_{\rm e}^{R,\eta}$.

singularity of the limit problem $\mathfrak{s}$, which obviously satisfies $\mathfrak{K}^R \geqslant \mathfrak{s}$ (using a maximum principle in $\Omega_{\rm i}^R$). For $\delta > 0$, the integrals

$$I_\bullet^\delta(R) = \frac{2}{\pi}\int_0^\pi \Big[\mathfrak{z}_\bullet^R(R-\delta,\theta) - \mathfrak{s}(R-\delta,\theta) - \mathfrak{l}(R-\delta,\theta)\Big]\mathfrak{s}^\star(R,\theta)\,\mathrm{d}\theta,$$

$$I^\delta(R) = \frac{2}{\pi}\int_0^\pi \Big[\mathfrak{K}_{\rm i}^R(R-\delta,\theta) - \mathfrak{s}(R-\delta,\theta) - \mathfrak{l}(R-\delta,\theta)\Big]\mathfrak{s}^\star(R,\theta)\,\mathrm{d}\theta,$$

$$I_0^\delta(R) = \frac{2}{\pi}\int_0^\pi \Big[\mathfrak{s}(R-\delta,\theta) - \mathfrak{s}(R-\delta,\theta) - \mathfrak{l}(R-\delta,\theta)\Big]\mathfrak{s}^\star(R,\theta)\,\mathrm{d}\theta,$$

satisfy $I^\delta(R) \geqslant I_0^\delta(R)$. Besides, there exists a point $\mathbf{x}_0$ such that $|\mathbf{x}_0| = R-\delta$ and $\mathfrak{K}^R(\mathbf{x}_0) > \mathfrak{s}(\mathbf{x}_0)$ (otherwise, all points satisfying $|\mathbf{x}| = R-\delta$ are critical points of the harmonic function $\mathfrak{K}^R - \mathfrak{s}$). We deduce that $I^\delta(R) > I_0^\delta(R)$. By uniform convergence of $I_\bullet^\delta(R)$ to $I_0(R)$ as $\delta \to 0$ and $\rho_\bullet \to \infty$, we obtain that there exist $\rho_\bullet$ and $c_\alpha > 0$ such that $I(R) \geqslant I_\bullet(R)$. ■

5.1.2 Numerical simulations

In the theoretical proofs above, we have shown that there exist a value of $\rho_\bullet$ such that the error $\|u_{\rm i}^\varepsilon - v_\bullet^\varepsilon\|_{\mathrm{L}^2(\Omega_{\rm i})}$ is $\mathcal{O}\big(\varepsilon^{\frac{3}{2}}\log^2(\varepsilon)\big)$ (instead of $\mathcal{O}(\varepsilon)$ for the standard Robin impedance condition). Actually, assumptions have been needed on the parameters ε_0 (thickness of the rescaled layer, see Figure 2) and c_α (defining the coefficient $\alpha_\bullet$, see Figure 4). Both have to be small enough, without any constructive information. The numerical simulations, however, will show that $\varepsilon_0 = 1$ and $c_\alpha = \frac{\alpha}{2}$ are admissible values.

Figure 7 presents the mapping $\rho_\bullet \mapsto \lambda_\bullet$ (actually $\lambda_\bullet^R$ computed via a finite element computation with FreeFem++ [36]).

It appears clearly that there exists a value $\rho_\bullet \simeq 0.2$ such that $\lambda_\bullet = \mu$. It is expected that for this very value of $\rho_\bullet$, the L^2-error between the solution of the transmission problem u^ε and the solution of the modified Robin impedance condition is of order $\varepsilon^{\frac{3}{2}}\log^2\varepsilon$.

We have performed simulations with varying values of $\rho_\bullet$, and computed the rate of convergence τ of the quantity $\|u_{\rm i}^\varepsilon - v_\bullet^\varepsilon\|_{\mathrm{L}^2(\Omega_{\rm i})} = \mathcal{O}(\varepsilon^\tau)$ as $\varepsilon \to 0$. The obtained results are presented on Figure 8, where the rate τ is plotted with respect to $\rho_\bullet$. We observe the expected improvement for the L^2 norm near the determined value of $\rho_\bullet$. Of course, the H^1 rate of convergence remains unchanged. Indeed, if the coefficients at infinity $\lambda_\bullet$ and μ are equal, the profiles $\mathfrak{z}_\bullet$ and $\mathfrak{K}$ themselves remain different. Their contribution lead to the H^1-norm in $\mathcal{O}(\sqrt{\varepsilon})$.

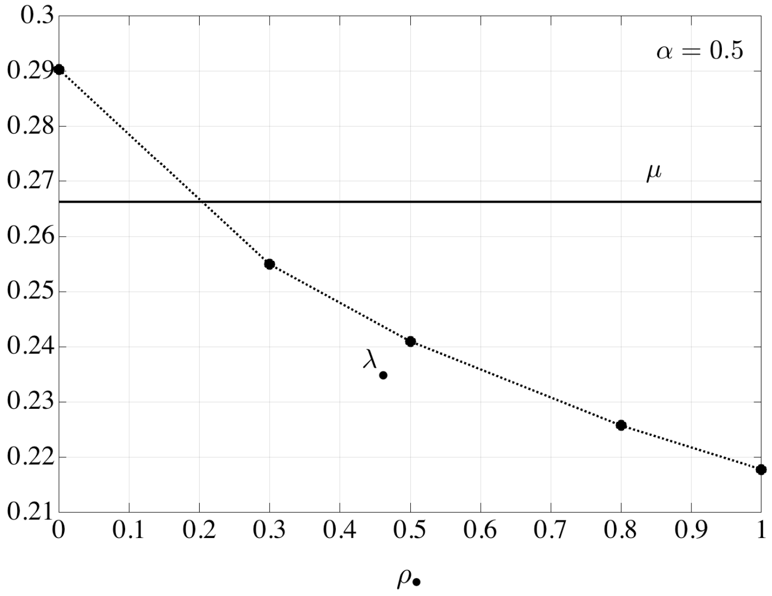

Figure 7: The graph of the mapping $\rho_\bullet \mapsto \lambda_\bullet$.

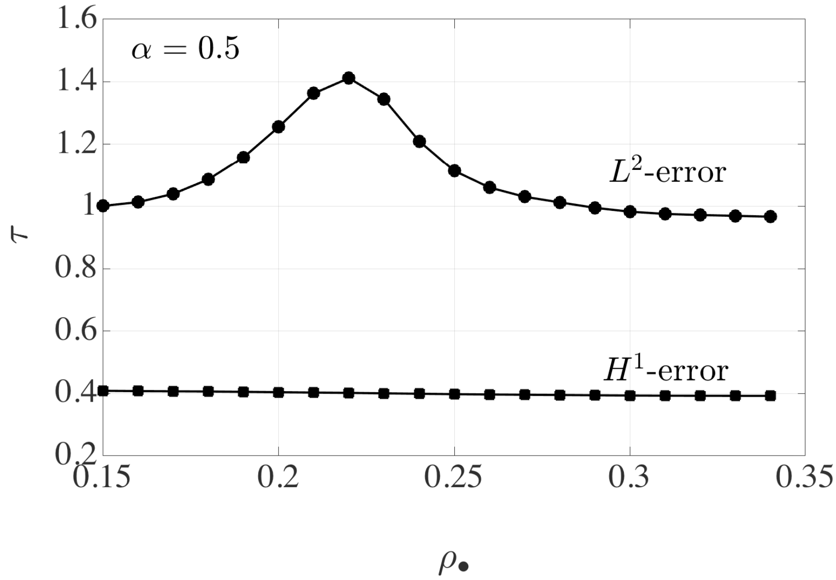

Figure 8: L^2 and H^1 rates of convergence of $u_{\mathrm{i}}^{\varepsilon} - v_{\bullet}^{\varepsilon}$ with respect to $\rho_\bullet$.

5.2 Ventcel impedance condition

The same idea can be exploited by introducing the following Ventcel problem.

$$\left\{\begin{array}{rcll} -\alpha\Delta v^{\varepsilon}_{\beta} &=& f_{\mathrm{i}} & \text{in } \Omega_{\mathrm{i}}, \\ \partial_{\nu} v^{\varepsilon}_{\beta} &=& 0 & \text{on } \Gamma_{\mathrm{N}}, \\ v^{\varepsilon}_{\beta} + \varepsilon\alpha\partial_{\nu} v^{\varepsilon}_{\beta} - \varepsilon^2\beta\partial^2_{\tau} v^{\varepsilon}_{\beta} &=& 0 & \text{on } \Gamma. \end{array}\right. \tag{22}$$

Problem (22) is well-posed in the variational space $\mathsf{V}_{\mathrm{v}} = \left\{ v \in \mathrm{H}^1(\Omega_{\mathrm{i}})\ ;\ v\big|_{\Gamma} \in \mathrm{H}^1(\Gamma) \right\}$ for $\beta > 0$. Once again, the techniques developed above allow to build an asymptotic expansion of v^{ε}_{β} with respect to ε. It take the form

$$\begin{aligned} v^{\varepsilon}_{\beta}(\mathbf{x}) = u^0(\mathbf{x}) + \gamma\chi(\mathbf{x})\sqrt{\varepsilon}(\mathfrak{z}_{\beta} - \mathfrak{s})\left(\tfrac{\mathbf{x}}{\varepsilon}\right) + \varepsilon u_{1,0}(\mathbf{x}) + \gamma\lambda_{\beta}\varepsilon u_{1,1}(\mathbf{x}) + \varepsilon u_1(\mathbf{x}) \\ + \varepsilon \log\varepsilon u_{1,2}(\mathbf{x}) + \mathcal{O}_{\mathrm{H}^1(\Omega_{\mathrm{i}})}\left(\varepsilon^{\frac{3}{2}} \log^2 \varepsilon\right), \end{aligned}$$

with a profile $\mathfrak{z}_{\beta}$ solving the homogeneous problem

$$\left\{\begin{array}{rcll} -\alpha\Delta\mathfrak{z}_{\beta} &=& 0 & \text{in } \Omega^{\infty}_{\mathrm{i}}, \\ \mathfrak{z}_{\beta} + \partial_{\nu}\mathfrak{z}_{\beta} - \beta\partial^2_{\tau}\mathfrak{z}_{\beta} &=& 0 & \text{on } \Gamma^{\infty}, \\ \partial_{\nu}\mathfrak{z}_{\beta} &=& 0 & \text{on } \Gamma^{\infty}_{\mathrm{N}}, \\ \mathfrak{z}_{\beta} &=& \mathfrak{s} + o(\sqrt{r}) & \text{at infinity}, \end{array}\right. \tag{23}$$

and admitting the following behavior at infinity

$$\mathfrak{z}_{\beta}(\mathbf{X}) = \mathfrak{s}(\mathbf{X}) + \mathfrak{l}(\mathbf{X}) + \lambda_{\beta}\,\mathfrak{s}^{\star}(\mathbf{X}) + \mathcal{O}\left(|\mathbf{X}|^{-\frac{3}{2}} \log^2(|\mathbf{X}|)\right). \tag{24}$$

The question is the following: can we find a value of β such that $\lambda_{\beta} = \mu$ (and hence the L^2-error between u^{ε} and v^{ε}_{β} is improved). No monotonicity for the profiles $\mathfrak{z}_{\beta}$ is true inside $\Omega^{\infty}_{\mathrm{i}}$. Nevertheless, the simulations performed seem to indicate that the mapping $\beta \mapsto \lambda_{\beta}$ is decreasing, and has μ in its range, but we are not able to prove it.

Again, the simulations are in rather good concordance. An improvement of the L^2 rate of convergence is observed near the optimal value of β, see Figures 9 and 10. The Ventcel condition does not involve a multiscale boundary condition, which is an advantage compared to the modified Robin impedance condition.

6 Profile correction

In the previous two sections, we have proposed modifications of the impedance condition, which allow to improve the rate of convergence in the L^2-norm. However, there is no improvement for the H^1-norm which remains $\mathcal{O}(\sqrt{\varepsilon})$. We present here a method of *profile correction* similar to [23, 13, 25]. The idea consists in pre-computing the profiles $\mathfrak{K}$ and $\mathfrak{z}$, and to build the correction

$$\tilde{v}^{\varepsilon}(\mathbf{x}) = v^{\varepsilon}(\mathbf{x}) + \gamma\sqrt{\varepsilon}(\mathfrak{K} - \mathfrak{z})\left(\tfrac{\mathbf{x}}{\varepsilon}\right),$$

which gives a better approximation of $u^{\varepsilon}_{\mathrm{i}}$ in the H^1-norm. Precisely,

$$\|u^{\varepsilon}_{\mathrm{i}} - \tilde{v}^{\varepsilon}(\mathbf{x})\|_{\mathrm{H}^1(\Omega_{\mathrm{i}})} = \mathcal{O}(\varepsilon).$$

Note that no improvement can be expected for the L^2-norm since the term $(\mu - \lambda)u_{1,1}$ is not modified in expression (13) for $\tilde{v}^{\varepsilon}$. The simulations presented in Figure 11 are consistent with these results.

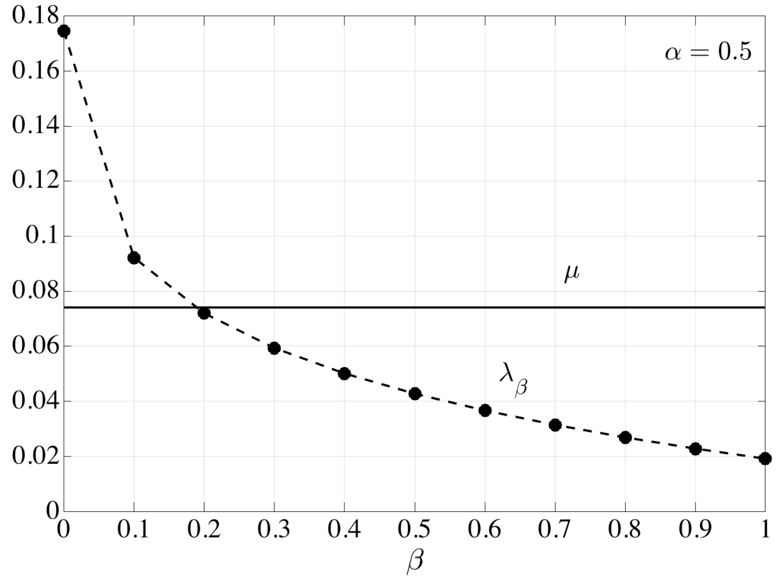

Figure 9: The graph of the mapping $\beta \mapsto \lambda_\beta$.

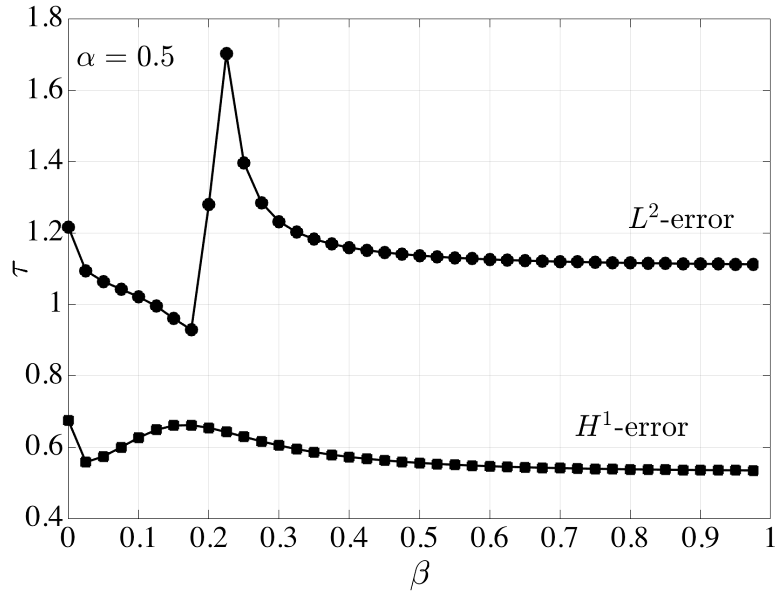

Figure 10: L^2 and H^1 rates of convergence of $u_{\mathrm{i}}^{\varepsilon} - v_{\beta}^{\varepsilon}$ with respect to β.

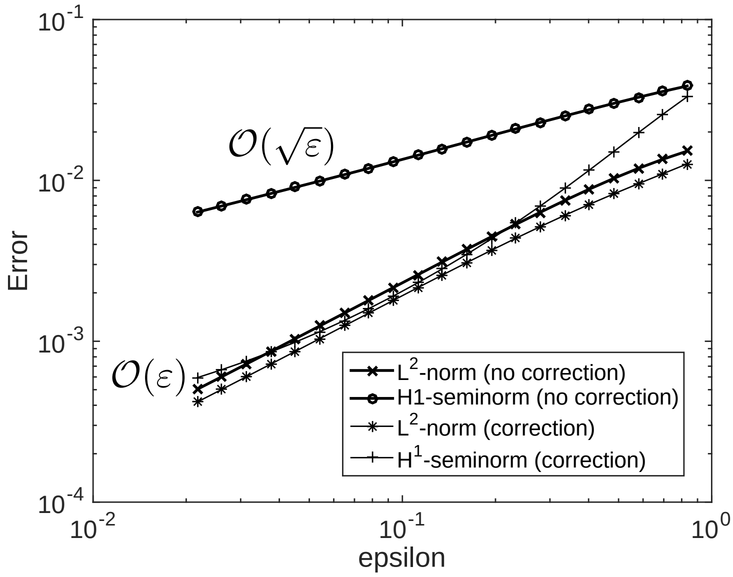

Figure 11: Errors $\|u^\varepsilon - v^\varepsilon\|$ and $\|u^\varepsilon - \tilde{v}^\varepsilon\|$ inside Ω_i with respect to ε.

7 Concluding remarks

In this paper, we have proposed two modifications of the standard Robin impedance condition, which appear to improve the L^2 rate of convergence to the transmission problem. The first one is a *multiscale Robin* condition, and a theoretical analysis of its performance has been developed, confirmed by numerical simulations. For the second one, of *Ventcel* type, very few theoretical arguments are available, but the numerical simulations are quite satisfactory. In both case, we can regret that the energy norm (i.e. H^1) is not improved. But the H^1-norm is related to the values of the profiles in the whole domain, not only to their behavior at infinity. A multiscale correction has been briefly presented which allows to decrease the energy rate of convergence, but requires the pre-computation of the profiles.

The presented methods extend to other boundary conditions, for example Neumann boundary conditions on the external boundary of the layer (but some proofs of Section 5.1.1 cannot be adapted). Let us mention that $3D$ computations have been performed to test the modified impedance conditions, in the case of a domain with an edge (but no corner). The extension operates well. We emphasize that the optimal values of $\rho_\bullet$ and β do not depend on the position along the edge. Simulations with corner domains in dimension 3 are underway.

Altogether, the improvements presented in this article may appear as rather modest. Indeed, they concern the very simple problem of the Laplace equation in 2 dimensions and the rates of convergence for the smooth case are far of being recovered. But they constitute a first step in that direction.

References

[1] M. V. ABDELKADER, A. A. MOUSSA. Asymptotic study of thin elastic layer. *Applied Mathematical Sciences* **7**(108) (2013) 5385–5396.

[2] E. ACERBI, G. BUTTAZZO. Reinforcement problems in the calculus of variations. *Ann. Inst. H. Poincaré Anal. Non Linéaire* **3**(4) (1986) 273–284.

[3] Y. ACHDOU, O. PIRONNEAU, F. VALENTIN. Effective boundary conditions for laminar flows over periodic rough boundaries. *Journal of Computational Physics* **147**(1) (1998) 187 – 218.

[4] H. AMMARI, E. BERETTA, E. FRANCINI. Reconstruction of thin conductivity imperfections. *Applicable Analysis* **83**(1) (2004) 63–76.

[5] H. AMMARI, S. HE. Effective impedance boundary conditions for an inhomogeneous thin layer on a curved metallic surface. *IEEE Transactions on Antennas and Propagation* **46**(5) (May 1998) 710–715.

[6] H. AMMARI, C. LATIRI-GROUZ. Approximate boundary conditions for thin periodic coatings. In *Mathematical and numerical aspects of wave propagation (Golden, CO, 1998)*, pages 297–301. SIAM, Philadelphia, PA 1998.

[7] H. T. ANASTASSIU, D. I. KAKLAMANI, D. P. ECONOMOU, O. BREINBJERG. Electromagnetic scattering analysis of coated conductors with edges using the method of auxiliary sources (mas) in conjunction with the standard impedance boundary condition (sibc). *IEEE Transactions on Antennas and Propagation* **50**(1) (Jan 2002) 59–66.

[8] A. AUVRAY, G. VIAL. Asymptotic expansions and effective boundary conditions : a short review for smooth and nonsmooth geometries with thin layers, to appear in ESAIM Proc., 2018.

[9] A. BASSON, D. GÉRARD-VARET. Wall laws for fluid flows at a boundary with random roughness. *Comm. Pure Appl. Math.* **61**(7) (2008) 941–987.

[10] M. BELLIEUD, G. GEYMONAT, F. KRASUCKI. Asymptotic analysis of a linear isotropic elastic composite reinforced by a thin layer of periodically distributed isotropic parallel stiff fibres. *J. Elasticity* **122**(1) (2016) 43–74.

[11] A. BENDALI, K. LEMRABET. The effect of a thin coating on the scattering of a time-harmonic wave for the Helmholtz equation. *SIAM J. Appl. Math.* **56**(6) (1996) 1664–1693.

[12] A. BENDALI, J.-R. POIRIER. Scattering by a highly oscillating surface. *Math. Methods Appl. Sci.* **38**(13) (2015) 2785–2802.

[13] V. BONNAILLIE-NOËL, D. BRANCHERIE, M. DAMBRINE, S. TORDEUX, G. VIAL. Effect of micro-defects on structure failure : coupling asymptotic analysis and strong discontinuity approach. *Eur. J. Comp. Mech* **10**(1,2,3) (2010) 165–175.

[14] M. BONNET, A. BUREL, M. DURUFLÉ, P. JOLY. Effective transmission conditions for thin-layer transmission problems in elastodynamics. The case of a planar layer model. *ESAIM Math. Model. Numer. Anal.* **50**(1) (2016) 43–75.

[15] C. D. BROWN, R. J. PHILLIPS. Crust-mantle decoupling by flexure of continental lithosphere. *Journal of Geophysical Research: Solid Earth* **105**(B6) (2000) 13221–13237.

[16] X. CAI, J. XU. Interface models for thin interfacial layers. *Appl. Math. Mech. (English Ed.)* **37**(6) (2016) 707–724.

[17] G. CALOZ, M. COSTABEL, M. DAUGE, G. VIAL. Asymptotic expansion of the solution of an interface problem in a polygonal domain with thin layer. *Asymptot. Anal.* **50**(1-2) (2006) 121–173.

[18] Y. CAPDEBOSCQ, M. S. VOGELIUS. Pointwise polarization tensor bounds, and applications to voltage perturbations caused by thin inhomogeneities. *Asymptot. Anal.* **50**(3-4) (2006) 175–204.

[19] Y. CAPDEVILLE, J.-J. MARIGO. Shallow layer correction for spectral element like methods. *Geophysical Journal International* **172**(3) (2008) 1135.

[20] F. CAUBET, H. HADDAR, J.-R. LI, D. V. NGUYEN. New Transmission Condition Accounting For Diffusion Anisotropy In Thin Layers Applied To Diffusion MRI. *Modelisation Mathématique et Analyse Numérique* (2016).

[21] M. COSTABEL, M. DAUGE. A singularly perturbed mixed boundary value problem. *Comm. Partial Differential Equations* **21** (1996) 1919–1949.

[22] M. DAMBRINE, I. GREFF, H. HARBRECHT, B. PUIG. Numerical solution of the homogeneous Neumann boundary value problem on domains with a thin layer of random thickness. *J. Comput. Phys.* **330** (2017) 943–959.

[23] M. DAMBRINE, G. VIAL. A multiscale correction method for local singular perturbations of the boundary. *M2AN Math. Model. Numer. Anal.* **41**(1) (2007) 111–127.

[24] M. DAUGE. *Elliptic Boundary Value Problems in Corner Domains – Smoothness and Asymptotics of Solutions*. Lecture Notes in Mathematics, Vol. 1341. Springer-Verlag, Berlin 1988.

[25] M. DAUGE, P. DULAR, L. KRÄHENBÜHL, V. PÉRON, R. PERRUSSEL, C. POIGNARD. Corner asymptotics of the magnetic potential in the eddy-current model. *Math. Methods Appl. Sci.* **37**(13) (2014) 1924–1955.

[26] B. DELOURME, H. HADDAR, P. JOLY. Approximate models for wave propagation across thin periodic interfaces. *J. Math. Pures Appl. (9)* **98**(1) (2012) 28–71.

[27] J. DIAZ, V. PÉRON. Equivalent Robin boundary conditions for acoustic and elastic media. *Math. Models Methods Appl. Sci.* **26**(8) (2016) 1531–1566.

[28] B. ENGQUIST, J. C. NEDELEC. Effective boundary conditions for electromagnetic scattering in thin layers. Rapport interne 278, CMAP 1993.

[29] M. M. S. FAKHRABADI, N. KHANI. Investigation of interphase effects on mechanical behaviors of carbon nanocone-based composites. *Mechanics & Industry* **15**(4) (001 2014) 287–292.

[30] S. GAJJELA, V. RAMACHANDRAN, J. SOMASEKHARAN. Influence of interphase material and clay particle shape on the effective properties of epoxy-clay nanocomposites. *Composites Part B: Engineering* **88** (2016) 11 – 18.

[31] G. GEYMONAT, F. KRASUCKI, S. LENCI. Mathematical analysis of a bonded joint with a soft thin adhesive. *Math. Mech. Solids* **4**(2) (1999) 201–225.

[32] D. GIVOLI. Finite element modeling of thin layers. *Comput. Model. Eng. Sci.* **5** (2004) 497 – 514.

[33] P. GRISVARD. *Boundary value problems in non-smooth domains*. Pitman, London 1985.

[34] H. HADDAR, Z. JIANG. Axisymmetric eddy current inspection of highly conducting thin layers via asymptotic models. *Inverse Problems* **31**(11) (2015) 115005.

[35] H. HADDAR, P. JOLY, H. NGUYEN. Generalized impedance boundary conditions for scattering problems from strongly absorbing obstacles: The case of maxwell's equations. *Mathematical Models and Methods in Applied Sciences* **18**(10) (2008) 1787–1827.

[36] F. HECHT. New development in freefem++. *J. Numer. Math.* **20**(3-4) (2012) 251–265.

[37] S. R. H. HOOLE. Experimental validation of the impedance boundary condition and a review of its limitations. *IEEE Transactions on Magnetics* **25**(4) (Jul 1989) 3028–3030.

[38] W. JÄGER, A. MIKELIĆ. On the roughness-induced effective boundary conditions for an incompressible viscous flow. *Journal of Differential Equations* **170**(1) (2001) 96 – 122.

[39] V. A. KONDRAT′EV. Boundary value problems for elliptic equations in domains with conical or angular points. *Trans. Moscow Math. Soc.* **16** (1967) 227–313.

[40] J. LI, S. ROSENCRANS, X. WANG, K. ZHANG. Asymptotic analysis of a Dirichlet problem for the heat equation on a coated body. *Proc. Amer. Math. Soc.* **137**(5) (2009) 1711–1721.

[41] G. M. LIEBERMAN. Local estimates for subsolutions and supersolutions of oblique derivative problems for general second order elliptic equations. *Trans. Amer. Math. Soc.* **304**(1) (1987) 343–353.

[42] R. PERRUSSEL, C. POIGNARD. Asymptotic expansion of steady-state potential in a high contrast medium with a thin resistive layer. *Applied Mathematics and Computation* **221** (2013) 48 – 65.

[43] C. POIGNARD. Boundary layer corrections and generalized polarization tensor for periodic rough thin layers. A review for the conductivity problem. In *Mathematical and numerical approaches for multiscale problem*, volume 37 of *ESAIM Proc.*, pages 136–165. EDP Sci., Les Ulis 2012.

[44] C. POIGNARD. Boundary layer corrections and generalized polarization tensor for periodic rough thin layers. A review for the conductivity problem. In *Mathematical and numerical approaches for multiscale problem*, volume 37 of *ESAIM Proc.*, pages 136–165. EDP Sci., Les Ulis 2012.

[45] O. P. POLYANSKY, S. N. KOROBEYNIKOV, V. G. SVERDLOVA, A. V. BABICHEV, V. V. REVERDATTO. The influence of crustal rheology on plate subduction based on numerical modeling results. *Doklady Earth Sciences* **430**(2) (2010) 158–162.

[46] L. PROEKT, S. YUFEREV, I. TSUKERMAN, N. IDA. Method of overlapping patches for electromagnetic computation near imperfectly conducting cusps and edges. *IEEE Transactions on Magnetics* **38**(2) (Mar 2002) 649–652.

[47] G. L. RICHARD, C. RUYER-QUIL, J. P. VILA. A three-equation model for thin films down an inclined plane. *Journal of Fluid Mechanics* **804** (10 2016) 162–200.

[48] K. SCHMIDT, A. CHERNOV. A unified analysis of transmission conditions for thin conducting sheets in the time-harmonic eddy current model. *SIAM J. Appl. Math.* **73**(6) (2013) 1980–2003.

[49] E. TUNCER, D. P. NEIKIRK. Efficient calculation of surface impedance for rectangular conductors. *Electronics Letters* **29**(24) (Nov 1993) 2127–2128.

[50] P. VERMA, P. MAIRE, P. NOVÁK. A review of the features and analyses of the solid electrolyte interphase in li-ion batteries. *Electrochimica Acta* **55**(22) (2010) 6332 – 6341.

[51] G. VIAL. Analyse multi-échelle et conditions aux limites approchées pour un problème de couche mince dans un domaine à coin. Thèse de doctorat 2840, Université de Rennes I, IRMAR 2003.

[52] G. VIAL. Efficiency of approximate boundary conditions for corner domains coated with thin layers. *CR. Acad. Sci.* **340** (January 2005) 215–220.

[53] S. YUFEREV, N. IDA. *Surface Impedance Boundary Conditions: A Comprehensive Approach*. CRC Press 2009.

[54] H. ZHAO, Z. YAO. Boundary conditions for the Stokes fluid in a bounded domain with a thin layer. *Kinet. Relat. Models* **9**(4) (2016) 797–812.

[55] D. D. ZUTTER, L. KNOCKAERT. Skin effect modeling based on a differential surface admittance operator. *IEEE Transactions on Microwave Theory and Techniques* **53**(8) (Aug 2005) 2526–2538.